Proceedings World Geothermal Congress 2020+1
Reykjavik, Iceland, April - October 2021

# Geothermal Fluids Isotope Characteristics in Xianyang Geothermal field, China

LUO Lu[1], PANG Zhonghe[2], Mao Xiang[1], ZHU Xia[1], HE Chunyan[1]

1. SINOPEC Star Petroleum., LTD, Beijing, China, 100083；

2. Institute of Geology and Geophysics, Chinese Academy of Sciences, 19 Beituchengxilu, Chaoyang district, Beijing, China, 100029

luolu_1989@163.com

**Keywords:** isotope, geothermal fluids, Xianyang

## ABSTRACT

Xianyang geothermal field is one of the largest areas for the development of geothermal energy in Guanzhong Basin, China. This paper mainly discusses the isotope characteristics of geothermal fluids in Xianyang geothermal field, including the $^2$H, $^{18}$O and $^{14}$C in geothermal water and noble gas isotopes in dissolved gases. The isotope $^{18}$O content of geothermal water in Xianyang geothermal field has obvious oxygen isotope shift tendency, which is the result of temperature, water-rock ratio and groundwater residence time. The isotope $^{14}$C content of geothermal water in Xianyang geothermal field is mostly low, the highest is 23pmc, and some water samples are lower than the detection limit. At the same time, according to the ratio of $^3$He / $^4$He and $^4$He / $^{20}$Ne of the noble gas isotope in geothermal water dissolved gas, it is proved that the Weibei fault in the Xianyang geothermal field only takes the thermal material of the crust. The circulation depth of the fluids is only within the depth of the crust.

## 1. INTRODUCTION

Guanzhong Basin is located between the Qinling Mountain in the south, the North Mountain in the north, and the Yellow River in the east. The geothermal reserves of Guanzhong Basin are large. In 1984, there were only 23 low-medium temperature natural springs and 37 geothermal wells in the region (Xu and Liang, 1984). However, by 2007, 346 geothermal wells were drilled with space heating area of 3.5 million m$^2$ (Pang et al., 2010). By the end of 2016, only a total of 105 geothermal wells and 8 recharge wells in Xianyang, and urban geothermal water extraction volume could reach 709.55×10$^4$ m$^3$ / a (Chen et al.,2018)

As the amount of geothermal water extraction increases year by year, and the geothermal water recharge work in this area progresses slowly, the sustainable development and utilization of geothermal resources will be affected. In order to better understand the large-scale exploitation of geothermal resources, it is necessary to clearly the characteristics of geothermal fluids. Previous studies have demonstrated that the recharge source of geothermal waters in Guanzhong Basin was precipitation during the last glacial period, in which Xianyang geothermal waters were recharged from the North Mountain (Tao, 2001; Qin and Tao, 2001; Ma et al., 2008; Li et al., 2012). However, Xianyang is located on two sides of the lithologic boundary; therefore the geothermal fluids characteristics and geothermal conditions may show different characteristics between the two sides. This paper will analyze the isotope characteristics of geothermal fluids.

## 2. STUDY AREA

The basement of Guanzhong Basin has large diversity in lithology, and Weibei Fault is the lithologic boundary(Fig.1). Weibei Fault controls the development of the basin and the boundaries of the adjacent tectonic units. During the Paleozoic period, the south of Weibei Fault was in the status of uplift and erosion. The east side of the fault is Archean metamorphic rock and the west is upper Proterozoic metamorphic rock. Meanwhile, the north of Weibei Fault formed a depression, which is comprised of the lower Paleozoic clastic and carbonate rock. The effect of Caledonian movement, formed the northern margin fault of the Guanzhong basin was formed. Because of the Mesozoic Indosinian movement and magmatism in the phase of Yanshan, the mountains of Qinling and Cou'e were uplifted gradually. The EW-trends squeeze broken belts were formed and the 8,000 km$^2$ of Yanshan granites were intruded in basement of the Guanzhong Basin. The radioactive uranium decay could form the total heat of 9.4×10$^{22}$ MJ and only 16% of uranium has decayed (Li and Xu, 2009). On the other hand, the depths of Moho and Curie in Xianyang are ~32 km and ~20 km, respectively. Xianyang is in mantle uplift area with a good geothermal background and a high heat flow background (Jiang et al., 2019). Radioactive uranium decay and mantle uplift are the main reasons for the formation of Xianyang geothermal field.

Three geothermal reservoirs have been identified and are being exploited from 800 to 4000 m (Fig.2). They are Neogene formations of Zhangjiapo, Lantianbahe and Gaoling group. The three reservoirs are sandstone intercalated with mudstone and are the main exploited at depth intervals of 800-1500 m, 1500-2700 m, and 2700-3200 m.

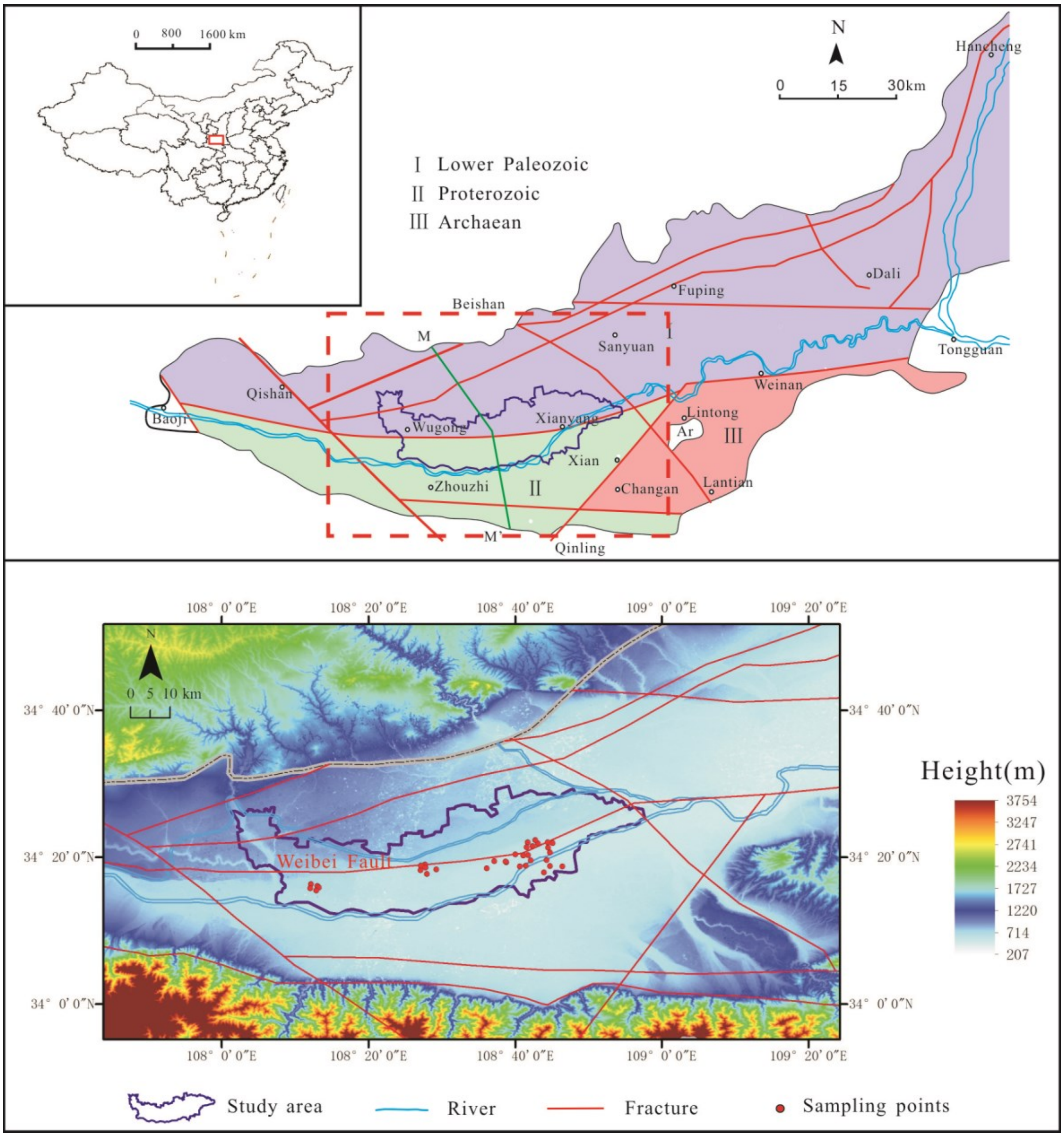


**Figure 1: Geological structures and sampling locations of the Xianyang geothermal field**

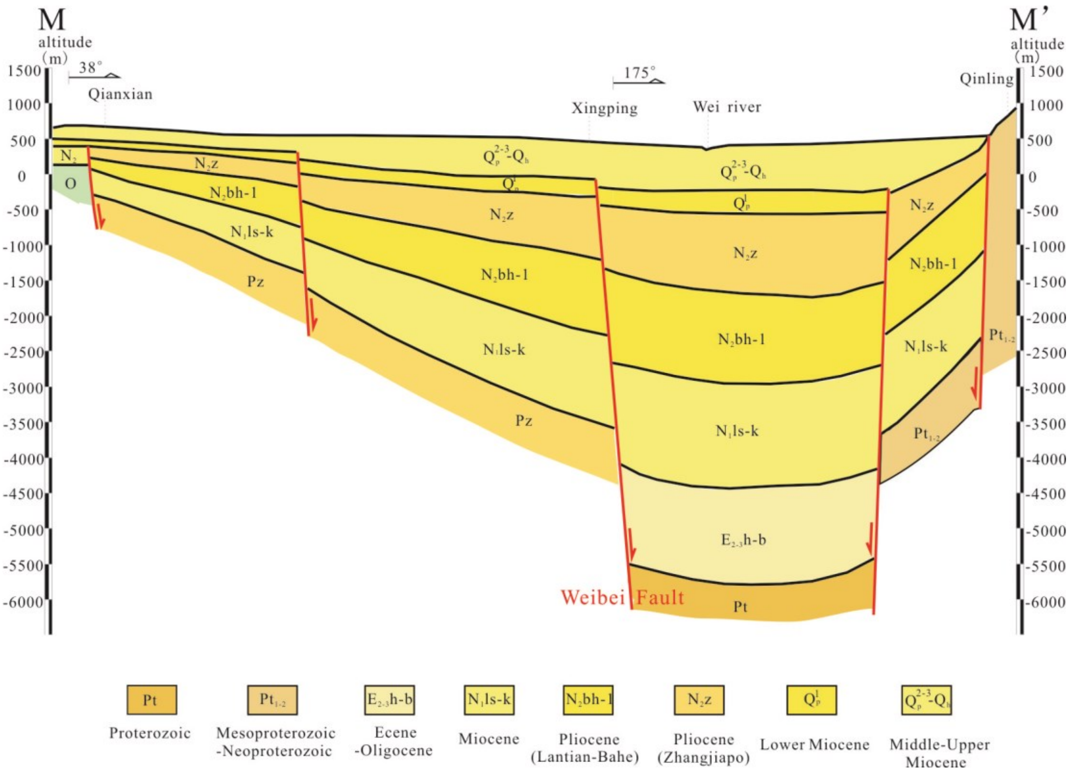


**Figure 2: Geothermal geological profile of study area (the location of M-M' profile is in Fig.1)**

## 3. SAMPLES AND METHODS

In order to carry out the analysis of the genesis of geothermal fluids in Xianyang, 35 geothermal water samples were collected in March 2018, and five dissolved gas samples were collected in March 2013. The distribution of sampling points is shown in Figure 1. It is mainly concentrated in the urban district of Xianyang. In addition, there are 5 sampling points in Wugong and 7 sampling points in Xingping（it is located between the urban district of Xianyang and Wugong）. The results of isotope test are shown in Table 1&2.

Physical and chemical parameters like pH, temperature, conductivity and Eh were measured in situ using a multi-parameter device HACH SENSION.The hydrogen-oxygen stable isotope of dissolved water and $^{13}C$ and $^{14}C$ of dissolved inorganic carbon (DIC) were tested in the Beta Analytic laboratory in the United States using gas-bench IRMS isotope mass spectrometry and accelerator mass spectrometry (AMS). The $^{14}C$ test accuracy is ±0.2 pmC (percent modern carbon); hydrogen-oxygen stable isotope and $^{13}C$ results are based on the Vienna Standard Average Ocean Water (VSMOW) with $\delta^{13}C$, $\delta D$ and $\delta^{18}O$ ($\delta$=(Rsample /Rstandard - 1) ×1000 ‰), the analysis accuracy is: $\delta^{13}C$ is ±0.3‰, $\delta D$ is ±2‰, and $\delta^{18}O$ is ±0.3‰.

Dissolved noble gases were sampled by negative pressure method (Luo et al., 2014; Arnozrsson et al., 2006 ), and analyzed using noble gas isotope mass spectrometer (MM5400) at Lanzhou Center for Oil and Gas Resources, Institute of Geology and Geophysics, Chinese Academy of Sciences. The accuracy is <3％.The sensitivity is $2\times10^{-4}$ (He, trap current=800 μA) and $1\times10^{-3}$ (Ar, trap current=200μA).

## 4. RESULTS AND DISCUSSION

### 4.1 Hydrogen and oxygen stable isotope characteristics of geothermal water

The hydrogen and oxygen stable isotope of Xianyang geothermal water has no obvious difference on both sides of the Weibei fault, but there is significant difference on oxygen isotope value changes (Table 1). In the $\delta D$-$\delta^{18}O$ plot (Fig. 3), a significant "oxygen isotope shift" occurs in the $\delta^{18}O$ value of geothermal water. This phenomenon is mostly found in high-temperature geothermal fields, and there are few such phenomena in low-temperature geothermal fields (Bolognesi et al., 2011; Bian et al., 2018; Tian et al., 2018). The "oxygen isotope shift" value generally depends on the initial content of $^{18}O$ in rock and geothermal water, lithology, thermal reservoir temperature, rock and water contact duration, and aquifer properties, and thermal reservoir temperature and contact duration are the most important factors (Pang et al., 2010; Qin et al., 2005). In medium-low temperature geothermal fields, there is strong evidence for the "oxygen isotope shift" in the Guanzhong Basin due to the long duration of contact between rocks and water (> 30000 yr). Therefore, it is suggested that the main cause of oxygen isotope shift in Xianyang may be the long contact time between water and rock. In addition, oxygen isotope shift values can be divided into two groups. The $\delta^{18}O$ value of group A was lower than -7 ‰, and that of group B was higher than -6 ‰. According to the drilling report, the mining thermal reservoirs of Group A are Zhangjiapo and Lantian Bahe Formation, and Group B is Lantian Bahe and Gaoling Group, indicating that the deeper the circulation depth, the longer circulation time will lead to higher oxygen isotope shift.

Isotope analysis indicates that geothermal water is derived from atmospheric precipitation. Comparing the $\delta D$ value of geothermal water with other groundwater in Guanzhong Basin, it shows that: 1) Qinling and Beishan are the main recharge sources in Guanzhong Basin, but the altitude of Beishan is much lower than that of Qinling, and the stable isotope of precipitation is depleted as altitude increases. Therefore, the hydrogen and oxygen stable isotope of the piedmont area in Qinling Mountains is more depleted than that of the northern basin (Fig. 3); 2) The groundwater in the piedmont area of Qinling Mountains in the southern basin is more depleted than the karst geothermal water in the northern basin, indicating that they are not from the same recharge source. 3) Xianyang geothermal water is similar to Xi'an geothermal water, and there is oxygen isotope shift phenomenon and δD values are similar. Previous studies have proved that geothermal water in the southern basin, especially Xi'an geothermal water, is supplied from the Qinling Mountains (Qin et al., 2005; Ma et al., 2005). At the same time, the δD value of Xianyang geothermal water is similar to the δD value of groundwater in the south of the basin. Therefore, based on the results of hydrogen and oxygen stable isotope, it can be concluded that Xianyang geothermal water is recharged from the Qinling Mountains.

**Table 1: The δD and δ18O value of geothermal water in study area**

| Location | Well | $\delta^{18}O$ (‰) | δD (‰) | Location | Well | $\delta^{18}O$ (‰) | δD (‰) |
|---|---|---|---|---|---|---|---|
| North of Weibei Fault | WR3 | -2.8 | -85.62 | South of Weibei Fault | EY | -3.2 | -85.9 |
| | WR5 | -3.98 | -84.86 | | SP2 | -2.8 | -83.5 |
| | WR7 | -5.6 | -86.13 | | J3 | -2.61 | -85.09 |
| | WR1 | -5.29 | -85.22 | | SP1 | -2.59 | -85.45 |
| | WR2 | -5.31 | -84.58 | | J2 | -1.87 | -86.24 |
| South of Weibei Fault | XR | -7.97 | -86.51 | | ZY1 | -7.4 | -88.87 |
| | ML | -7.52 | -84.62 | | HYJC1 | -11.1 | -85.65 |
| | HT | -3.91 | -85.52 | | JCJY1 | -8.9 | -83.85 |
| | DZH1 | -9.92 | -84.89 | | JCJY2 | -9.1 | -85.21 |
| | SXHP1 | -7.5 | -86.43 | | WGX1 | -10.2 | -83.52 |
| | FRJY1 | -3.3 | -86.01 | | WG3 | -8.89 | -82.71 |
| | QLY1 | -8.8 | -86.53 | | WG2 | -9.7 | -84.56 |
| | J1 | -3.14 | -87.46 | | | | |

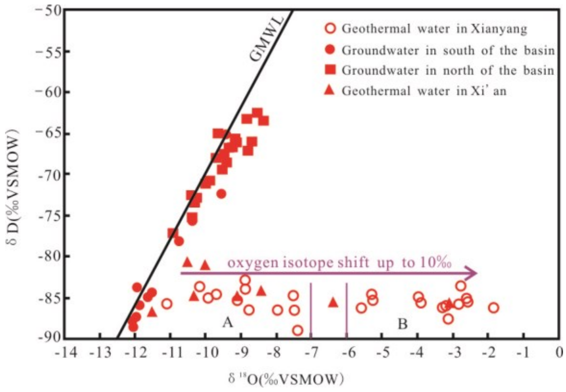


**Figure 3: δD-$\delta^{18}O$ plot showing the stable isotope composition of the thermal waters in Guanzhong Basin. The solid line is the Global Meteoric Water Line (GMWL), $\delta D=8\delta^{18}O+10$. The groundwater data except Xianyang geothermal water were cited from Qin et al., 2005 and Ma et al., 2006.**

### 4.2 $^{14}C$ and $^{13}C$ isotope characteristics

The $^{14}C$, $\delta^{13}C$ content and the corrected model age of the geothermal water in Xianyang area are as shown in Table 2.The $\delta^{13}C$ value was used to calculate the pearson corrected age. The age of Xianyang geothermal water is more than 16ka, and some water samples even exceed the detection limit of $^{14}C$. The age is greater than 43ka, which is in the last glacial period of the Quaternary in northern China. The distribution of the $^{14}C$ content is shown in Fig 4. It can be seen that there is no significant difference in the ages on both sides of the Weibei fault. The geothermal water age of Wugong is obviously smaller than that of the urban district of Xianyang. Its renewal ability is also faster than that of the urban district of Xianyang. The smaller age of the four wells on the east side of the urban district of Xianyang is caused by the shallow depth of the well.

**Table 2: The 14C and δ13C values, apparent ages and corrected ages of study area**

| Well | Middle section depth of reservoir (m) | $^{14}C$ (pMC) | $\delta^{13}C$ (‰) | Apparent radiocarbon age (year) | Pearson corrected age (year) |
|---|---|---|---|---|---|
| SXHP1 | 2496 | < 0.44 | -7.7 | >43500 | >43500 |
| FRJY1 | 2711 | < 0.44 | -3.2 | >43500 | >43500 |
| QLY1 | 1582 | < 0.44 | -7 | >43500 | >43500 |

| | | | | | |
|---|---|---|---|---|---|
| EY | - | 0.5 | -5.9 | 43799 | 33321 |
| SP2 | 1655 | 3.5 | -5.5 | 27713 | 16726 |
| ZY1 | 3100 | 1.9 | -5.5 | 32763 | 21776 |
| WR7 | 2196 | 0.5 | -7.1 | 43799 | 34683 |
| J2 | 2360 | 3 | -10.3 | 28260 | 22682 |
| J1 | 3614 | 1.2 | -8 | 35380 | 28337 |
| WR4 | 2134 | 5.2 | -12.9 | 23710 | 19875 |
| DZH1 | 1511 | 1.3 | -12.3 | 34890 | 30965 |
| XR | 2030 | 2.8 | -11.6 | 28710 | 24168 |
| HYJC1 | 2111 | 0.6 | -9.2 | 42292 | 35124 |
| JCJY1 | 2406 | 1.6 | -6.5 | 34184 | 24414 |
| XTJY | 2080 | < 0.44 | -6.2 | >43500 | >43500 |
| WG2 | 2268 | 23 | -18.6 | 11800 | 10459 |

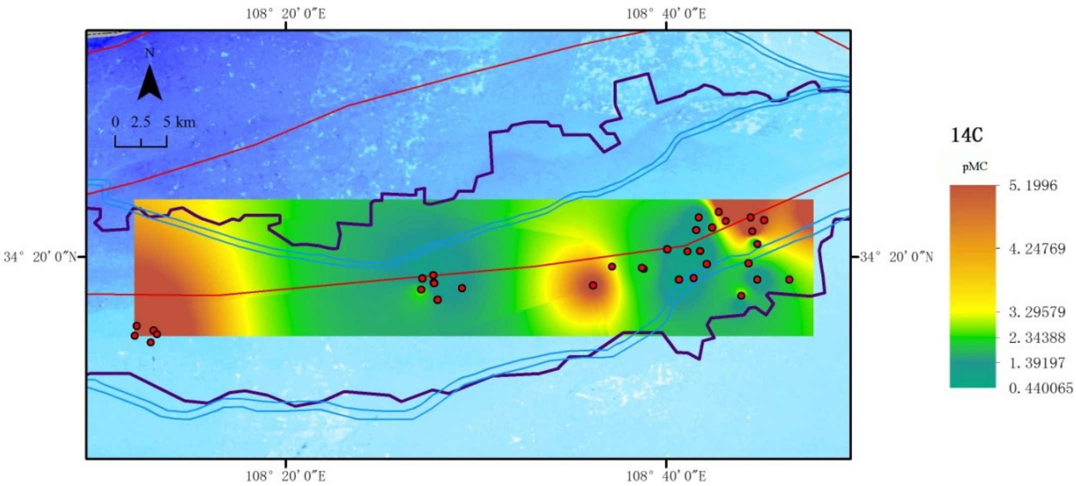


**Figure 4: The distribution map of $^{14}$C value in study area**

**4.3 Noble gas isotope characteristics**

The noble gas can be used in geothermal research for identifying source, mixing and crust-mantle fluids interaction (Craig, 1976; Poreda & Craig 1989; Fischer et al., 2009; Zhou et al., 2012). Helium isotope provides clear evidence for volatiles from mantle origin in geothermal systems, and indicates the role of heat sources and mantle melting in the formation of geothermal systems (Dallai et al., 2005; Arnorsson et al., 2006; Darrah et al., 2013). On the $^{3}$He/$^{4}$He-$^{4}$He/$^{20}$Ne diagram, the mixing line between air, mantle and crust can be calculated using the formula in Craig et al. (1976). The lower $^{3}$He/$^{4}$He value corresponds to a higher $^{4}$He/$^{20}$Ne value indicating that the diversity of He content and the low value of $^{3}$He/$^{4}$He are not due to atmospheric dilution. The range of $^{3}$He/$^{4}$He values is the result of various mixing between the $^{3}$He-rich mantle fluid and the $^{4}$He-rich crustal fluid. The relationship between the $^{3}$He / $^{4}$He and $^{4}$He / $^{20}$Ne ratios of dissolved hot gas in the study area is shown in Fig.5. Fig.5 shows that the dissolved gas in the Xianyang geothermal water has a lower $^{3}$He / $^{4}$He ratio and a higher $^{4}$He / $^{20}$Ne ratio, close to the crust value, inferring that the geothermal gas comes from the crust or a mixture of crust and air, there are no mantle source. Therefore, it is proved that the circulation depth of the Xianyang geothermal fluid is within the depth range of the crust.

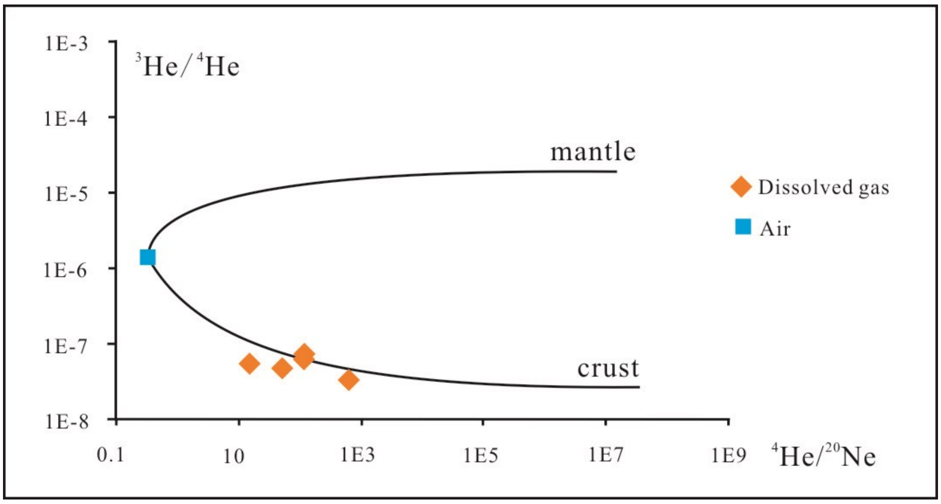


**Figure 5: $^{3}He/^{4}He$-$^{4}He/^{20}Ne$ plots of the dissolved gas in geothermal water**

## 5. CONCLUSION

The hydrogen and oxygen isotopes of geothermal water in the Xianyang geothermal field have the characteristics of atmospheric origin, but the oxygen isotope shift occurs after the interaction of water and rock. This phenomenon indicates the older geothermal age, and also shows that the sedimentary environment of Guanzhong Basin had resulted that the groundwater flowing slowly. The $^{14}C$ contents of some geothermal water is low, which is close to or exceeds the detection limit of the instrument. It is recommended to use other dating methods to study the geothermal water in Guanzhong Basin. In the dissolved gas of Xianyang geothermal water, the ratio of $^{3}He$ / $^{4}He$ is low and the ratio of $^{4}He$ / $^{20}Ne$ is high. It is concluded that the geothermal gas comes from the earth's crust or a mixture of crust and air, no mantle source.

## REFERENCES

Verma, A., and Pruess, K.: Enhancement of Steam Phase Relative Permeability Due to Phase Transformation Effects in Porous Media, *Proceedings,* 11th Workshop on Geothermal Reservoir Engineering, Stanford University, Stanford, CA (1986). <Reference Style>

Wang, C.T., and Horne, R.N.: Boiling Flow in a Horizontal Fracture, *Geothermics*, **29**, (1999), 759-772. <Reference Style>

Arnorsson S., Bjarnason J. O., Giroud N., et al.: Sampling and analysis of geothermal fluids, *Geofluids*, **6**,(2006), 203-216.

Dallai L., Magro G., Petrucci E., et al.: Stable isotope and noble gas isotope compositions of inclusion fluids from Larderello geothermal field (Italy): Constraints to fluid origin and mixing processes. *Journal of Volcanology and Geothermal Research*, **148**, (2005), 152-164.

Darrah T. H., Tedesco D., Tassi F., et al.: Gas chemistry of the Dallol region of the Danakil Depression in the Afar region of the northern-most East African Rift, *Chemical Geology*, **339,** (2013), 16-29.

Bian Y. Y., Zhao D.: Genesis of Geothermal Waters in the Kangding Geothermal Field, Sichuan Province, *Acta Geoscientica Sinica*, **39(4),** (2008), 491-497.

Bolognesi L.: The oxygen isotope exchange between carbon dioxide and water in the Larderello geothermal field(Italy) during fluid reinjection, *Geothermics*, **40**, (2011), 181-189.

Chen Y. Q., Ji Y. T., Pu J. Y., et al.: Discussion on development patterns of middle and deep geothermal resources in Guanzhong Basin, *West-China Exploration Engineering*, **(11)**, (2018), 103-106

Craig H., Lupton J. E.: 1976. Primordial neon, helium, and hydrogen in oceanic basalts, *Earth and Planetary Science Letters*, **31 (3)**, (1976), 369–385.

Fischer T. P., Burnard P., Martyb B., et al.: Upper-mantle volatile chemistry at Oldoinyo Lengai volcano and the origin of carbonatites, *Nature*, **459 (7243**), (2009), 77–80.

Jiang G. Z., Hu S. B., Shi Y. Z., et al.: Terrestrial heat flow of continental China: Updated dataset and tectonic implications, *Tectonophysics*, **753**, (2019), 36-48.

Li T., Hu W. W., Ma Z. Y., et al.: Enviromental isotope evidences of recharge of geopressured geothermal waters in Xianyang, *Geotechnical Investigation&Surveying*, **(2)**, (2012), 47-50.

Li Z. L.，Xu C. J.: Geological research of Weihe Fault Basin and Xianyang geotherm, *Zhongzhou Coal*, **(11)**, (2009), 9-11&58.

Luo L., Pang Z. H., Luo J., et al.: Noble gas isotopes to determine in the depth of the geothermal fluid circulation, *Chinese Journal of Geology*, **49(3)**, (2014), 888-898.

Ma Z. Y., Fan J. J., Niu G. L., et al.: 2005. Classification of thermal water in Guanzhong Area, Shannxi Province, *Coal Geology&Exploration*, **33(5)**, (2005), 54-57.

Ma Z. Y., Fan J. J., Su Y., et al.:Hydrogeology significance on hydrogrn and oxygen isotopes composition in underground thermal water of Guanzhong area, Shannxi provinxe, *Jounal of Earth Sciences and Environmen*t, **28(1)**, (2006), 41-46.

Ma Z. Y., Yu J., Li Q., et al.: Environmental isotope distribution and hydrologic geologic sense of Guanzhong Basin geothermal water, *Journal of Earth Sciences and Environment*, **30(4)**, (2008), 396-401.

Pang Z. H., Yang F. T., Huang T. M., et al.: Genesis analysis of geothermal system in Guanzhong Basin of China with implications on sustainable geothermal resources development, *Proceedings*, World Geothermal Congress, Bali, Indonesia (2010).

Poreda R., Craig H.: Helium isotope ratios in circum-Pacific volcanic arcs, *Nature*, **338 (6215)**, (1989), 473–478.

Qin D., Tao S. H.: Isotope constrains on the hydraulic relationship of groundwaters between Quaternary and Tertiary aquifer in Xi'an area, Shaanxi province, *Science in Chin*a, **44**, (2001), 72-79.

Qin D. J., Turner J. V., Pang Z. H.: Hydrogeochemistry and groundwater circulation in the Xi'an geothermal field, China, *Geothermics*, **34**, (2005), 471-494.

Tao S. H.: The source of replenishment of geothermal water around Xi'an, *Science in China*, **44**, (2001), 165-167.

Tian J., Pang Z. H., Guo Q., et al.: Geochemistry fluids with implications on sources of water and heat recharge on the Rekeng high-temperature geothermal system in the Eastern Himalayan Syntax, *Geothermics*, **74**, (2018), 92-105.

Xu J. G., Liang Y. S.: Types and characteristics of geothermal waters in Guanzhong Basin, *Hydrogeology and Engineering Geology*, **(2)**, (1984), 25-28.

Zhou Z., Ballentine C. J., Schoell M., et al.: Identifying and quantifying natural $CO_2$ sequestration processes over geological timescales: the Jackson Dome $CO_2$ Deposit, USA, *Geochimica et Cosmochimica Acta*, **86**, (2012), 257–275.